Dexmedetomidine attenuates sepsis-induced myocardial injury in association with TRPV1 upregulation and ferroptosis suppression

Juanjuan Miao,[1] Rui Tang,[1] Changyan Hu,[1] Ying Zhang,[2] Qihong Zhao[1]

[1]Department of Anesthesiology, The Second Affiliated Hospital of Bengbu Medical University, Bengbu, Anhui
[2]Department of Anesthesiology, The First Affiliated Hospital of Bengbu Medical University, Bengbu, Anhui, China

ABSTRACT

Sepsis-induced myocardial injury involves oxidative stress, iron dysregulation, and ferroptosis-related changes. The role of transient receptor potential vanilloid 1 (TRPV1) in mediating the cardioprotective effects of dexmedetomidine (DEX) remains to be elucidated. We evaluated DEX pretreatment in mice subjected to cecal ligation and puncture (CLP) and in lipopolysaccharide (LPS)-stimulated H9c2 cells, using capsaicin, capsazepine, and ferrostatin-1 (Fer-1) as pharmacological probes. A separate 5-day time-course cohort identified day 2 as the peak injury time point based on cardiac injury and biochemical markers, guiding subsequent experiments. In CLP mice, DEX pretreatment improved survival and cardiac function, attenuated myocardial histopathological injury, and reduced oxidative stress and iron accumulation. In H9c2 cells, DEX preserved cell viability and mitochondrial morphology, increased TRPV1, GPX4, and SLC7A11 expression, and decreased ACSL4 expression. Capsaicin reproduced several protective effects of DEX, whereas capsazepine partially attenuated these effects. Fer-1 improved ferroptosis-related indicators and also increased TRPV1 expression. Together, these findings demonstrate consistent DEX-associated protection across animal and cell models, accompanied by TRPV1 upregulation and reduced ferroptosis-related injury. The pharmacological findings support the involvement of TRPV1-sensitive signaling in this protective response.

Key words: dexmedetomidine; TRPV1; ferroptosis; lipopolysaccharide; sepsis.

Correspondence: Dr. Qihong Zhao, Department of Anesthesiology, The Second Affiliated Hospital of Bengbu Medical University; No. 633 Longhua Street, Huaishang District, Bengbu City, 233000, Anhui Province, China. E-mail: zhaoqh0516@163.com
Dr. Ying Zhang, Department of Anesthesiology, The First Affiliated Hospital of Bengbu Medical University; No. 287 Changhuai Street, Longzihu District, Bengbu City, 233004, Anhui Province, China. E-mail: underyin@163.com

Contributions: Juanjuan Miao, conceptualization, data curation, funding acquisition, formal analysis, investigation, methodology, writing-original draft. Rui Tang, conceptualization, data curation, formal analysis, investigation, methodology, writing-original draft. Changyan Hu, conceptualization, data curation, funding acquisition, formal analysis, investigation, methodology, writing-original draft. Ying Zhang, conceptualization, project administration, resources, supervision, validation, writing-review & editing. Qihong Zhao, conceptualization, funding acquisition, project administration, resources, supervision, validation, writing-review & editing. All authors have read and approved the final version of the manuscript.

Conflict of interest: the authors declare no competing interests and all authors confirm accuracy.

Ethical approval: this study was approved by the Ethics Committee of Bengbu Medical University (Approval number: 2024[391]).

Data Availability Statement: the data supporting this study are available from the corresponding author upon reasonable request.

Funding: this study was supported by the Key Natural Science Project of Bengbu Medical University (No. 2023byzd100), the “unveiling the list and leading the way" scientific research key task project of Bengbu Medical University (No. 2025byjbgs091), and the Guidance Project of Scientific and Technological Innovation of Bengbu City of Anhui Province (No. 2024ZD0022)

Introduction

Cardiovascular diseases remain the leading cause of mortality worldwide.[1] Their pathogenesis is intricately associated with myocardial cell injury, inflammatory responses, and cell death. Lipopolysaccharide (LPS)-induced myocardial inflammatory injury is a well-established model for studying pathological processes such as septic cardiomyopathy and ischemia-reperfusion injury.[2] These conditions can result in myocardial dysfunction through the activation of oxidative stress, mitochondrial dysfunction, and cell death pathways.[3] Therefore, investigating critical targets and developing intervention strategies to regulate myocardial cell survival is essential for enhancing the prognosis of cardiovascular diseases.

Dexmedetomidine (DEX), a highly selective α_2-adrenergic receptor activator, has gained recognition as a potential agent for myocardial protection.[4] In clinical settings, DEX is extensively utilized for sedation in intensive care units. Recent meta-analyses have indicated that DEX administration is associated with reduced serum concentrations of cardiac troponin I (cTnI) and creatine kinase-MB (CK-MB) in patients with sepsis, which correlates with enhanced hemodynamic stability.[5] Preclinical investigations have further corroborated the anti-inflammatory and antioxidant properties of DEX in rodent models of myocardial ischemia-reperfusion injury and sepsis. Nevertheless, the specific molecular mechanisms responsible for DEX's cardioprotective effects remain inadequately elucidated, particularly concerning its interactions with ion channels and cell death pathways.

Transient receptor potential vanilloid 1 (TRPV1) is a non-selective cation channel involved in vascular tone and blood flow regulation.[6] TRPV1 is abundantly expressed in cardiomyocytes, endothelial cells, and cardiac sensory nerves, where it influences calcium influx, reactive oxygen species (ROS) production, and mitochondrial dynamics.[7] Recent research underscores the dual role of TRPV1 in myocardial injury: while excessive activation can exacerbate calcium overload and oxidative stress, activation may also offer protection through anti-inflammatory signaling pathways.[8] Notably, TRPV1 knockout mice demonstrate increased susceptibility to myocardial ischemia-reperfusion injury, indicating that endogenous TRPV1 activation may have cardioprotective effects.[9] However, whether TRPV1-sensitive signaling contributes to DEX-associated protection in sepsis-induced myocardial injury remains unresolved.

Furthermore, ferroptosis, a recently identified iron-dependent form of regulated cell death, has emerged as a significant mediator of myocardial injury.[10] Ferroptosis, distinct from apoptosis and necrosis, is characterized by the inactivation of glutathione peroxidase 4 (GPX4), the accumulation of lipid peroxides (LPO), and mitochondrial shrinkage accompanied by a reduction in cristae.[11] In LPS-induced sepsis-induced myocardial dysfunction (SIMD), ferroptosis is initiated through the Toll-like receptor 4 (TLR4) mediated upregulation of acyl-CoA synthetase long-chain family member 4 (ACSL4) and the downregulation of the cystine-glutamate antiporter (SLC7A11), resulting in uncontrolled lipid peroxidation.[12] Although targeting ferroptosis, for instance, through GPX4 activators or iron chelators, has demonstrated efficacy in preclinical models, the regulation of ferroptosis by G protein-coupled receptors (GPCRs), such as α_2-adrenergic receptors, remains incompletely understood.

TRPV1 regulation and ferroptosis-related injury may intersect during DEX-associated cardioprotection.[13,14] We therefore established a 5-day CLP injury profile, identified the most informative time point for subsequent experiments, and assessed DEX pretreatment alongside pharmacological modulation with capsaicin, capsazepine, and Fer-1 in CLP mice and LPS-stimulated H9c2 cells. This paired model approach tests whether the changes in TRPV1 expression and ferroptosis-related indicators accompany a consistent protective phenotype.

Materials and Methods

Animals

Male C57BL/6 mice, aged 8-10 weeks and weighing 18-22 g, were procured from Hangzhou Ziyuan Laboratory Animal Science and Technology Co., Ltd. (Hangzhou, China; Laboratory Animal Production License No. SCXK [Zhe] 2024-0004). The mice were acclimatized for 7 days under specific pathogen-free (SPF) housing conditions, with a controlled temperature of 22±2°C, relative humidity of 50±10%, and a 12-h light-dark cycle. Throughout the experimental period, the mice were provided with sterile chow and autoclaved water *ad libitum*. All animal experiments were conducted in accordance with the ARRIVE guidelines and complied with the U.K. Animals (Scientific Procedures) Act 1986 and its associated guidelines, the EU Directive 2010/63/EU on the protection of animals used for scientific purposes, and the National Institutes of Health (NIH) Guide for the Care and Use of Laboratory Animals (NIH Publications No. 8023, revised 1978). Additionally, all animal studies were performed in strict compliance with the regulations and guidelines established by the Ethics Committee of Bengbu Medical University (Approval number: 2024[391]).

Sepsis modeling and experimental design

Sepsis was induced by cecal ligation and puncture (CLP). Mice were anesthetized with 3% isoflurane, a 1 cm midline abdominal incision was made, and the cecum was ligated at ~50% of its length from the ileocecal valve using a 6-0 silk suture, then punctured twice with a 21-gauge needle to extrude a small amount of feces. The cecum was returned to the abdominal cavity and the incision was closed. Sham-operated mice underwent the same procedure without ligation or puncture. All animals received postoperative subcutaneous saline (50 mL/kg) for fluid resuscitation.

For survival analysis, 80 mice were randomly allocated to Control (untreated), Sham, CLP, and CLP + DEX groups (n=20 per group). DEX (10 μg/kg, i.p.) was administered 30 min before CLP, and survival was monitored for 5 days.[15,16] A separate time-course cohort comprised 120 mice: Control (untreated), Sham, CLP, and CLP + DEX groups (n=30 per group). On each of days 1-5 after surgery, three mice per group were randomly selected for blood and heart collection for subsequent analyses. For mechanistic studies on day 2 post-CLP (the peak injury time point identified in the separate time-course cohort), a separate cohort of mice was randomly assigned to six groups (n=6/group): i) Control (untreated); ii) CLP; iii) CLP + DEX (10 μg/kg, i.p., 30 min prior to CLP); iv) CLP + Ferrostatin-1 (Fer-1, 1 mg/kg, i.p., 2 h prior to CLP, as a ferroptosis inhibition positive control);[17] v) CLP + Capsaicin (TRPV1 activator, 1 mg/kg, i.p., 1 h prior to CLP);[18] and vi) CLP + DEX + Capsazepine (TRPV1 inhibitor, 5 mg/kg, i.p., 30 min before DEX, followed by CLP 30 min later).[19]

Echocardiography

On day 2 post-surgery, cardiac function was evaluated using a high-resolution small-animal ultrasound system (Vevo 3100; FUJIFILM VisualSonics, Inc., Toronto, Canada). Mice were lightly anesthetized with isoflurane (1-1.5%) and placed supine on a heat-

OPEN ACCESS

ed platform. Left ventricular ejection fraction (LVEF) and fractional shortening (LVFS) were measured in M-mode from the parasternal long-axis view by an investigator blinded to group allocation, with values averaged from at least three consecutive cardiac cycles.

ELISA for serum cardiac biomarkers

Blood was collected via orbital venous plexus puncture on days 1-5 post-CLP. Serum was separated by centrifugation (3,000 × g, 15 min, 4°C) and stored at −80°C. Cardiac troponin I (cTnI) and CK-MB levels were measured using commercial ELISA kits (cTnI: E-EL-M1203; CK-MB: E-EL-M0355; Elabscience Bionovation, Inc., Wuhan, China) per the manufacturer's protocols. Absorbance was read at 450 nm (BioTek Synergy H1; BioTek Instruments, Winooski, VT, USA). Detection ranges were 7.81-500 pg/mL for cTnI and 78.13-5000 pg/mL for CK-MB.

Biochemical assays

Intracellular ferrous iron (Fe^{2+}) content was measured using an Iron Assay Kit (E-BC-K881-M, E-BC-K773-M; Elabscience Bionovation, Inc.). Glutathione (GSH) activity was determined using a GSH Assay Kit (E-BC-K030-M; Elabscience Bionovation, Inc.). Lipid peroxidation (LPO) levels were assessed using a Lipid Peroxidation Assay Kit (E-BC-K176-M, Elabscience). Malondialdehyde (MDA) levels were quantified using an MDA Assay Kit (E-BC-K028-M, Elabscience). Myocardial ROS levels were assessed by incubating tissue homogenate supernatants with dihydroethidium (DHE; S0063, Beyotime, China) at 37°C in the dark, followed by fluorescence measurement using a BioTek Synergy H1 microplate reader (Agilent, USA). All assays were performed according to the manufacturers' protocols.

Histopathological and immunohistochemical analyses

Heart tissues were fixed in 4% paraformaldehyde, paraffin-embedded, and sectioned at 4 μm. For H&E staining, sections were deparaffinized, rehydrated, stained with hematoxylin (5-10 min) and eosin (3-5 min), dehydrated, cleared, and mounted. Histopathological assessment was performed by an investigator blinded to group allocation. For immunohistochemistry (IHC), sections underwent antigen retrieval in citrate buffer (pH 6.0), quenching of endogenous peroxidase with 3% H_2O_2, and blocking with goat serum. Samples were then incubated with anti-GPX4 primary antibody (1:200, #52455, CST) at 4°C overnight, followed by HRP-conjugated secondary antibody (30 min, room temperature). Signals were visualized with DAB, counterstained with hematoxylin, and imaged using Pannoramic MIDI (3DHISTECH, Budapest, Hungary). Image acquisition was performed with investigators blinded to group allocation.

Cell culture and *in vitro* model

Rat embryonic cardiomyocyte H9c2 cells were cultured in high-glucose DMEM (Gibco, Waltham, MA, USA) supplemented with 10% FBS (10099-141; Gibco) and 1% penicillin-streptomycin (15140-122; Gibco) at 37°C in 5% CO_2. Cells were subcultured with 0.25% trypsin-EDTA (25200072; Gibco) at ~80% confluence. *In vitro* injury was induced by exposure to 10 μg/mL lipopolysaccharide (LPS) for 24 h.

Phase 1, designed to evaluate the effect of DEX on TRPV1, comprised three groups: Control, LPS, and LPS + DEX. Cells were stimulated with LPS (10 μg/mL) for 24 h.[20] DEX (1 μM) was administered 2 h before LPS stimulation.[21,22].

Phase 2, designed to assess the effects of pharmacological TRPV1 modulation on DEX-associated cytoprotection and ferroptosis-related changes, comprised six groups: Control, LPS, LPS + DEX (1 μM), LPS + Fer-1 (1 μM),[23] LPS + Capsaicin (10 μM; a TRPV1 agonist), and LPS + DEX + Capsazepine (10 μM; a TRPV1 antagonist). DEX and Fer-1 were administered 2 h before LPS stimulation,[24] whereas capsaicin and capsazepine were added 15 and 20 min before LPS stimulation, respectively.[25,26] Cells were subsequently exposed to LPS (10 μg/mL) for 24 h.

Cell viability

For cell viability assays, cells were seeded at 5 × 10^3 cells/well in 96-well plates and assigned to the treatment groups described in the "Cell culture and *in vitro* model" section. The medium was not replaced during the assay period. At 24, 48, 72, 96, and 120 h after the start of LPS treatment, 10 μL of CCK-8 reagent (CK04; Dojindo Laboratories, Kumamoto, Japan) was added to each well and incubated for 2 h at 37°C. Absorbance was measured at 450 nm.

Cellular ROS and immunofluorescence

Intracellular ROS was measured using DCFH-DA (D6883; Sigma-Aldrich, St. Louis, MO, USA). Treated cells were incubated with 10 μM DCFH-DA in serum-free medium for 20 min at 37°C, then analyzed by flow cytometry (BD FACSCanto II, 488/525 nm, 10,000 events/sample). The percentage of ROS-positive cells was quantified. For TRPV1 localization, cells on coverslips were fixed in 4% paraformaldehyde, permeabilized with 0.1% Triton X-100, blocked with 5% BSA, and incubated with anti-TRPV1 primary antibody (1:200) at 4°C overnight, followed by Alexa Fluor 488-conjugated secondary antibody (1:500) for 1 h at room temperature. Nuclei were counterstained with DAPI, and images were acquired using a Zeiss LSM 880 confocal microscope. Image acquisition and fluorescence quantification were performed with investigators blinded to group allocation.

Transmission electron microscopy

Cells were fixed in 2.5% glutaraldehyde (in 0.1 M PBS, pH 7.4) for 2 h at 4°C, post-fixed in 1% osmium tetroxide for 1 h, dehydrated in graded ethanol, and embedded in Epon 812. Ultrathin sections (70 nm) were stained with uranyl acetate and lead citrate, then examined under a JEOL JEM-1400Plus TEM at 80 kV. Mitochondrial morphology was analyzed using ImageJ by an investigator blinded to group allocation.

qRT-PCR

Total RNA was extracted using TRIzol™ (15596026; Invitrogen, Waltham, MA, USA). cDNA was synthesized from 1 μg RNA using PrimeScript RT Master Mix (RR036A; Takara Bio Inc., Kusatsu, Japan). qRT-PCR was performed on a StepOnePlus system (Applied Biosystems, Waltham, MA, USA) with SYBR Premix Ex Taq™ (RR420A, Takara). Cycling conditions: 95°C for 30 s, followed by 40 cycles of 95°C for 5 s and 60°C for 34 s. Relative mRNA expression was calculated using the 2^−ΔΔCt method with *Actb* as the internal control. All reactions were run in triplicate. The primer sequences were as follows: *Trpv1*, forward 5′-GCATCTTCTACTTCAACTTCTTCGTC-3′ and reverse 5′-CCACATACTCCTTGCGATGGC-3′; *Actb*, forward 5′-CGTTGACATCCGTAAAGAC-3′ and reverse 5′-CTGGAAGGTGGACAGTGAG-3′.

Western blotting

Cells or tissues were lysed in RIPA buffer (P0013B; Beyotime Biotechnology, Shanghai, China) containing protease and phos-

phatase inhibitors (Roche, Basel, Switzerland, and Sigma-Aldrich). Protein concentration was determined by BCA assay (23225; Thermo Fisher Scientific, Waltham, MA, USA). Equal amounts (30 µg) were separated by 10% SDS-PAGE and transferred to PVDF membranes (IPVH00010; Millipore, Burlington, MA, USA). Membranes were blocked with 5% non-fat milk in TBST, then incubated overnight at 4°C with primary antibodies against TRPV1 (1:1000, DF10320; Affinity Biosciences, Cincinnati, OH, USA), GPX4 (1:1000, #52455; Cell Signaling Technology, Danvers, MA, USA), ACSL4 (1:1000, 22401-1-AP; Proteintech), SLC7A11 (1:1000, PA1-16893; Invitrogen), and β-actin (1:5000, A5441; Sigma-Aldrich). After washing, membranes were incubated with HRP-conjugated secondary antibodies (1:5000, #7076; Cell Signaling Technology) for 1 h at room temperature. Bands were visualized using ECL substrate (WBKLS0500; Millipore) and quantified with ImageJ.

Statistical analysis

Data are presented as mean ±SD. Survival curves (n=20 per group) were analyzed using the Kaplan-Meier method and log-rank test. Each mouse in the separate Figure 1 B-G time-course cohort contributed one observation at one time point (n=3 mice per displayed group per day). Each biochemical outcome in Figure 1 B-G was analyzed separately using ordinary two-way ANOVA with treatment group, day, and their interaction as factors, followed by multiplicity-adjusted prespecified comparisons between treatment groups within each day. For the CCK-8 time-course assay, inferential testing was performed at the final prespecified observation time. Other independent-group outcomes were analyzed using one-way ANOVA followed by Tukey's multiple-comparisons test, as applicable. Statistical analyses were performed using GraphPad Prism 9.0; two-sided $p<0.05$ was considered significant.

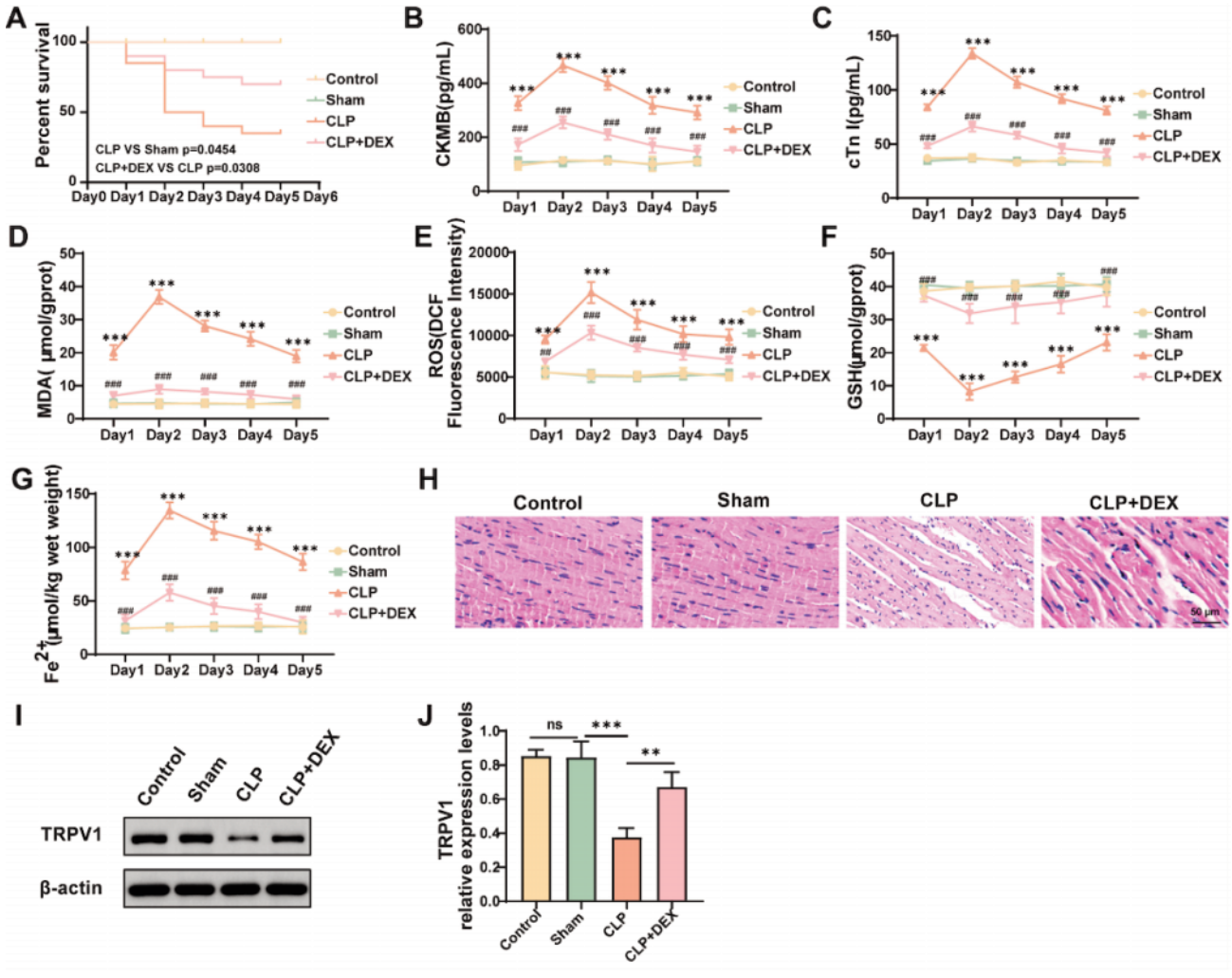

Figure 1. Time-course of CLP-induced myocardial injury and the protective effects associated with DEX pretreatment over 5 days after surgery. **A**) Kaplan-Meier survival curves from the independent survival cohort (n=20 per group). **B,C**) Serum CK-MB (**B**) and cTnI (**C**) measured by ELISA. D-G) Myocardial MDA (**D**), ROS (**E**), GSH (F), and Fe^{2+} (**G**); panels B–G were measured in a separate time-course cohort (n=3 independent mice per displayed group at each time point) and analyzed using ordinary two-way ANOVA with group, day, and their interaction. **H**) Representative H&E staining of myocardial tissue collected on day 2; scale bar: 50 µm. **I-J**) Representative Western blots (**I**) and quantitative analysis (**J**) of TRPV1 protein expression in myocardial tissue collected on day 2 (n=3 per group); $^{**}p<0.01$, $^{***}p<0.001$ *vs* Sham at the corresponding time point; $^{\#\#}p<0.01$, $^{\#\#\#}p<0.001$ *vs* CLP at the corresponding time point; (J) $^{**}p<0.01$, $^{***}p<0.001$; ns, not significant.

OPEN ACCESS

Results

Time-course of CLP-induced myocardial injury and protective effects of DEX

To define the temporal profile of sepsis-induced myocardial injury and select the most informative time point for mechanistic studies, we evaluated survival, serum biomarkers, oxidative stress markers, iron levels, histopathology, and TRPV1 expression over 5 days after CLP. CLP mice showed progressive mortality, whereas DEX pretreatment improved survival (Figure 1A). Serum CK-MB and cTnI, myocardial MDA, ROS, and Fe^{2+} reached their highest measured levels on day 2, while GSH reached its lowest level (Figure 1 B-G). Day-2 H&E staining showed marked disruption of myocardial architecture, inflammatory cell infiltration, and cardiomyocyte injury, which were attenuated by DEX pretreatment (Figure 1H). Western blot analysis of myocardial tissue collected on day 2 showed that CLP reduced TRPV1 protein expression compared with the Sham group ($p<0.001$), whereas DEX pretreatment increased TRPV1 expression compared with the CLP group ($p<0.01$; Figure 1I, J). The temporal profiles of cardiac injury and biochemical markers identified day 2 as the peak injury time point in this CLP model, supporting its selection for subsequent mechanistic experiments.

DEX mitigates oxidative stress in the CLP mouse model

Based on the time-course results identifying day 2 as the peak injury time point, all subsequent mechanistic experiments were performed on day 2 after CLP. CLP reduced GSH and increased MDA, Fe^{2+}, ROS, and LPO levels relative to the control group ($p<0.001$). DEX pretreatment, Fer-1, and capsaicin each shifted these measures toward control levels ($p<0.001$ *vs* CLP). Capsazepine partially reduced the effects of DEX ($p<0.001$ *vs* CLP + DEX; Figure 2 A-E). The concordant changes across multiple oxidative stress and ferroptosis-related measures support the involvement of TRPV1-sensitive signaling in DEX-associated cardioprotection.

DEX attenuates CLP-induced myocardial pathological alterations

Quantitative analysis (Figure 2F) confirmed that CLP significantly decreased LVEF and LVFS compared to the Control group ($p<0.001$), whereas DEX, Fer-1, or capsaicin treatment significantly improved these parameters ($p<0.01$ *vs* CLP). M-mode echocardiographic tracings (Figure 2G) showed that CLP markedly reduced left ventricular wall motion and chamber shortening, which was significantly restored by DEX pretreatment. As shown in Figure 2H, histopathological examination using H&E staining revealed significant pathological alterations in the CLP group compared to the control group. These alterations included disrupted cellular architecture, inflammatory cell infiltration. The pathological changes in the CLP group were characterized by an increased extent and severity of lesions. In contrast, the CLP + DEX, CLP + Fer-1, and CLP + capsaicin groups exhibited only slight pathological alterations, with largely intact tissue structures. Notably, the co-administration of capsazepine with DEX partially reversed the protective effect of DEX.

GPX4 immunostaining was weaker in the CLP group than in the Control group. Pretreatment with DEX, Fer-1, or capsaicin increased GPX4 staining, whereas capsazepine partially attenuated the effect of DEX (Figure 2I).

DEX modulates TRPV1/ACSL4/SLC7A11 levels in the CLP mouse model

Western blot analysis provided molecular evidence elucidating the underlying signaling mechanisms. Studies demonstrated a significant upregulation of ACSL4 protein expression in the CLP group compared to the control group ($p<0.001$). Conversely, the expression of TRPV1 and SLC7A11 were significantly downregulated relative to the Control group ($p<0.01$). These molecular alterations were notably reversed following treatment with DEX, Fer-1, or capsaicin ($p<0.01$ or $p<0.001$ *vs* CLP group). However, the concurrent administration of capsazepine partially reversed the effects of DEX ($p<0.01$ or $p<0.001$ *vs* CLP + DEX group; Figure 2 J-M).

DEX attenuates LPS-induced cytotoxicity in H9c2 cells

To assess the protective effects of DEX against LPS-induced cellular damage, cell viability was quantified using the CCK-8 assay. As shown in Figure 3A, treatment with LPS (10 μg/mL) significantly reduced H9c2 cell viability compared to the Control group ($p<0.001$). Co-treatment with DEX markedly reversed this reduction ($p<0.001$ *vs* LPS group). This indicated that DEX mitigates LPS-induced cytotoxicity in cardiomyocytes.

DEX upregulates TRPV1 expression in LPS-stimulated H9c2 cells

Subsequently, we investigated whether DEX influences TRPV1 expression under conditions of LPS-induced stress. qRT-PCR analysis revealed that exposure to LPS alone resulted in a significant downregulation of *TRPV1* mRNA levels when compared to the Control group ($p<0.001$), while co-treatment with DEX increased *TRPV1* mRNA expression ($p<0.01$ *vs* LPS group; Figure 3B). Western blotting consistently revealed that LPS significantly decreased TRPV1 protein levels ($p<0.01$ *vs* Control group), whereas co-treatment with DEX significantly upregulated TRPV1 protein expression ($p<0.05$ *vs* LPS group; Figure 3 C,D).

Pharmacological modulation of TRPV1 alters the protective effect of DEX on cell viability

To examine whether TRPV1-sensitive signaling contributes to the cytoprotective effect of DEX, we used capsaicin and capsazepine as pharmacological probes. Cell viability was higher in the LPS + DEX, LPS + Fer-1, and LPS + capsaicin groups than in the LPS group (all $p<0.001$; Figure 4A). Capsazepine partially reduced the protective effect of DEX ($p<0.001$ *vs* LPS + DEX). These findings provide pharmacological evidence that TRPV1-sensitive signaling contributes to the cytoprotective effect of DEX, as TRPV1 blockade by capsazepine partially reversed DEX-mediated protection.

TRPV1 pharmacological modulation influences the antioxidant effects associated with DEX

Oxidative stress is a key driver of LPS-induced myocardial injury. LPS increased LPO and MDA and reduced GSH activity (all $p<0.001$ *vs* Control). DEX, Fer-1, and capsaicin each shifted these measures toward control levels ($p<0.001$ *vs* LPS), whereas capsazepine diminished the effects associated with DEX ($p<0.001$ *vs* LPS + DEX; Figure 4 B-D). These data link the DEX-associated antioxidant phenotype to pharmacologically TRPV1-sensitive processes. Flow cytometry showed that LPS increased the percentage of ROS-positive cells compared with the Control group

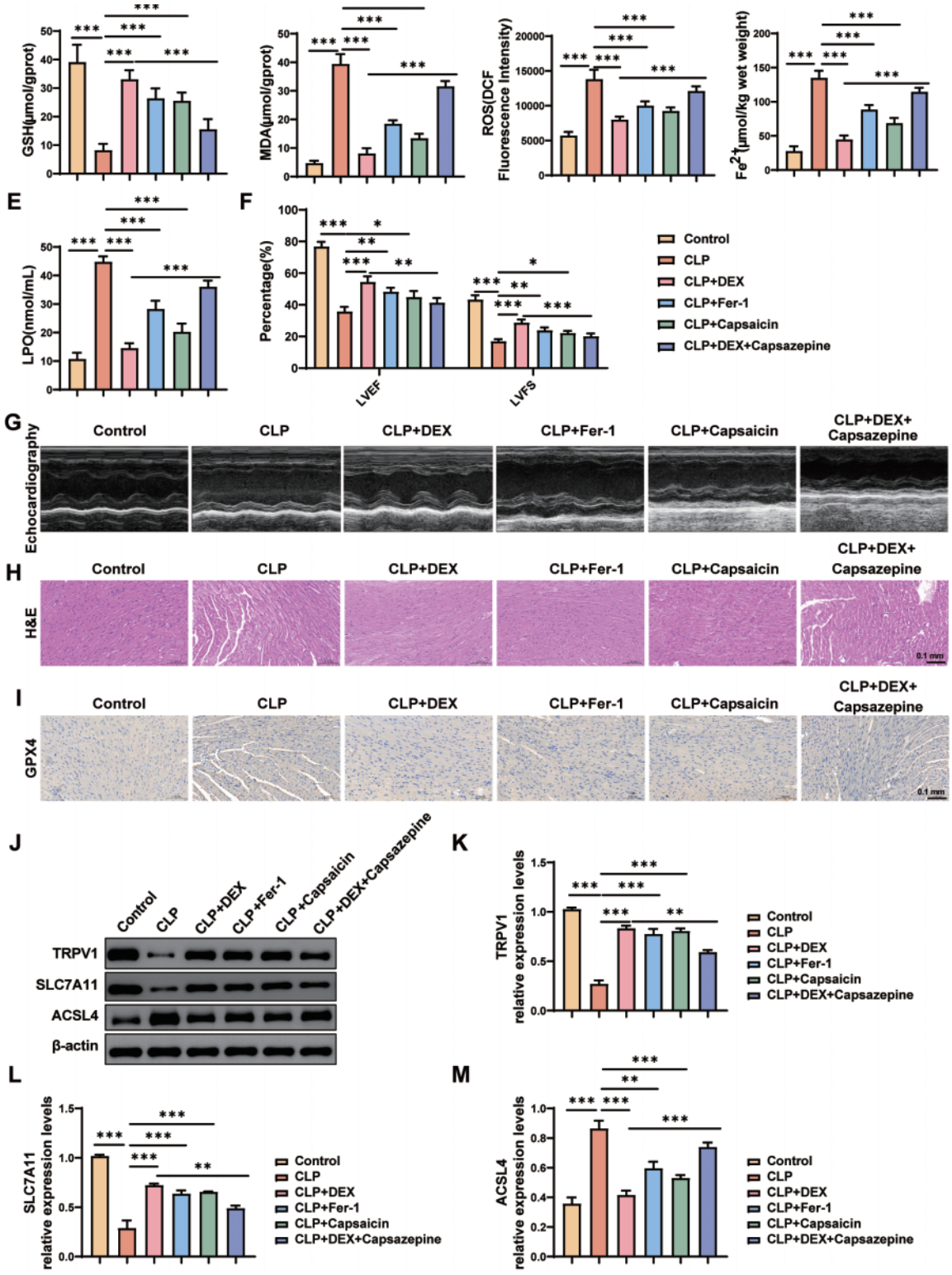

Figure 2. DEX ameliorates myocardial injury, cardiac dysfunction, oxidative stress, and ferroptosis-related protein expression in CLP mice. **A**) Quantitative analysis of GSH levels. **B**) Quantitative analysis of MDA levels. **C**) Quantitative analysis of ROS levels. **D**) Quantitative analysis of Fe^{2+} levels. **E**) Quantitative analysis of LPO levels. **F**) Quantitative analysis of left ventricular ejection fraction (LVEF) and left ventricular fractional shortening (LVFS) in each group. **G**) Representative M-mode echocardiographic tracings of the left ventricle. **H**) Representative images of hematoxylin and eosin (H&E) staining of myocardial tissue sections; scale bar: 0.1 mm). **I**) Representative images of immunohistochemical (IHC) staining of GPX4 in myocardial tissue sections; scale bar: 0.1 mm. **J**) Representative Western blotting images showing the protein levels of TRPV1, SLC7A11, and ACSL4 in each group, with β-actin as the loading control. **K-M**) Quantitative analysis of TRPV1 (K), SLC7A11 (L), and ACSL4 (M); Data are presented as mean ±SD (n=3 per group). *p<0.05, **p<0.01, ***p<0.001.

OPEN ACCESS

(p<0.001). DEX, Fer-1, and capsaicin reduced this percentage (p<0.001 *vs* LPS), whereas capsazepine partially attenuated the effect of DEX (p<0.001 *vs* LPS + DEX; Figure 4 E,F).

DEX modulates alterations in mitochondrial structure and TRPV1 expression/localization

Mitochondrial dysfunction is a hallmark of ferroptosis. We used TEM to assess mitochondrial morphology. In the control group, mitochondria exhibited intact cristae and normal structure. LPS stimulation induced typical ferroptosis-associated mitochondrial alterations, including mitochondrial shrinkage, increased membrane density, and cristae reduction/disappearance, whereas co-treatment with DEX, Fer-1, or capsaicin preserved normal mitochondrial ultrastructure (Figure 5A), with capsazepine partially reversing these effects.

Immunofluorescence staining showed TRPV1 expression (green fluorescence) and localization, with DAPI (blue) labeling nuclei. As shown in Figure 5 D-E, in the Control group, TRPV1 fluorescence was predominantly distributed throughout the cytoplasm. LPS treatment reduced TRPV1 fluorescence intensity with a more diffuse distribution pattern. LPS+DEX reversed LPS-induced suppression, showing significantly enhanced cytoplasmic TRPV1 fluorescence. LPS+Fer-1 moderately increased TRPV1 intensity. LPS+capsaicin group showed partially restored TRPV1 fluorescence intensity, comparable to that of the LPS+Fer-1 group. LPS+DEX+capsazepine reduced TRPV1 fluorescence intensity, indicating that capsazepine partially reversed DEX-mediated upregulation.

DEX is associated with reduced ferroptosis, TRPV1 upregulation, and modulation of the GPX4, ACSL4, and SLC7A11 expression

Because oxidative stress and iron accumulation are core features of ferroptosis, we examined intracellular Fe^{2+} and ferroptosis-related proteins. LPS increased Fe^{2+} levels (p<0.001 *vs* Control), whereas DEX, Fer-1, and capsaicin reduced Fe^{2+} accumulation (all p<0.001 *vs* LPS; Figure 5B). Capsazepine partially reduced the effect associated with DEX (p<0.001 *vs* LPS + DEX).

Western blotting showed that LPS reduced GPX4 and SLC7A11 and increased ACSL4 relative to the Control group (all p<0.001). DEX, Fer-1, and capsaicin shifted these proteins toward control levels, whereas capsazepine partially reduced the changes associated with DEX (p<0.05 *vs* LPS + DEX; Figure 6 A-E). Together with the biochemical and ultrastructural findings, these results support an association among DEX treatment, TRPV1-sensitive signaling, and suppression of ferroptosis-related changes.

Concurrently, qRT-PCR (Figure 5C) and Western blot assays (Figure 6B) were conducted to assess TRPV1 levels. The data demonstrated that LPS significantly reduced TRPV1 expression compared to the Control group (p<0.001). The expression of TRPV1 was restored by treatment with DEX, Fer-1, or capsaicin, whereas capsazepine partially reversed these effects (p<0.01 *vs* LPS + DEX group).

Discussion

This study demonstrates consistent DEX-associated protection in CLP mice and LPS-stimulated H9c2 cells, accompanied by TRPV1 upregulation and reduced ferroptosis-related injury. The 5-day profiles of cardiac injury and biochemical markers identified day 2 as the peak injury time point in the CLP model. DEX pretreatment improved cardiac function and myocardial tissue morphology and reduced oxidative stress and iron accumulation. In H9c2 cells, DEX preserved cell viability and mitochondrial morphology and shifted ferroptosis-related protein expression toward

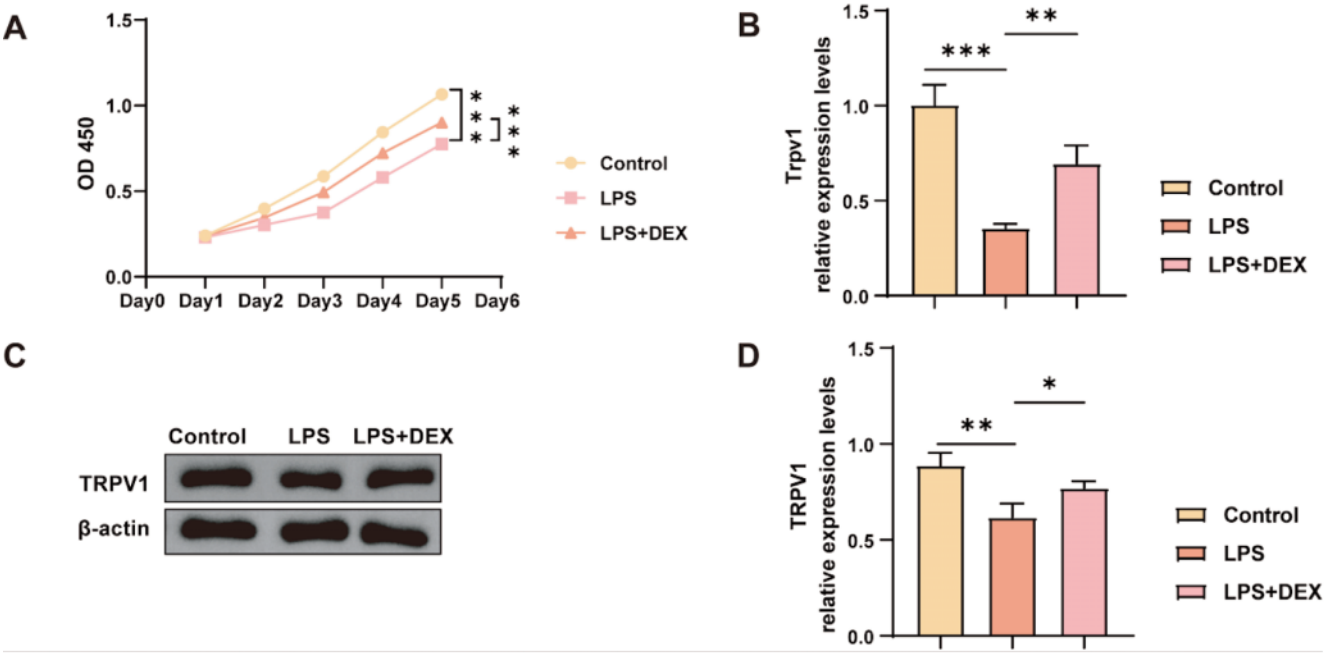

Figure 3. Co-treatment with DEX attenuates LPS-induced cytotoxicity and upregulates TRPV1 expression in H9c2 cells. **A**) Cell viability detected by CCK-8 assay. **B**) *TRPV1* mRNA expression measured by qRT-PCR. **C,D**) TRPV1 protein expression analyzed by Western blot; representative blots (**C**) and quantitative analysis (**D**); Data are presented as mean ±SD (n=3 per group). *p<0.05, **p<0.01, ***p<0.001.

control levels. Capsaicin reproduced several protective effects, whereas capsazepine partially attenuated the effects of DEX. Together, these findings provide pharmacological support for the involvement of TRPV1-sensitive signaling in the protective response.

Previous studies have shown that DEX can protect against myocardial ischemia-reperfusion injury by attenuating ferroptosis in cardiomyocytes.[27,28] DEX also influences endothelial and immune-cell function,[29,30] both of which can shape myocardial injury.[31] The present study extends this evidence by showing concordant protection in CLP mice and LPS-stimulated H9c2 cells. Across both systems, DEX increased TRPV1 expression while reducing oxidative stress, iron accumulation, and ferroptosis-related changes. The cellular findings support a direct cardiomyocyte

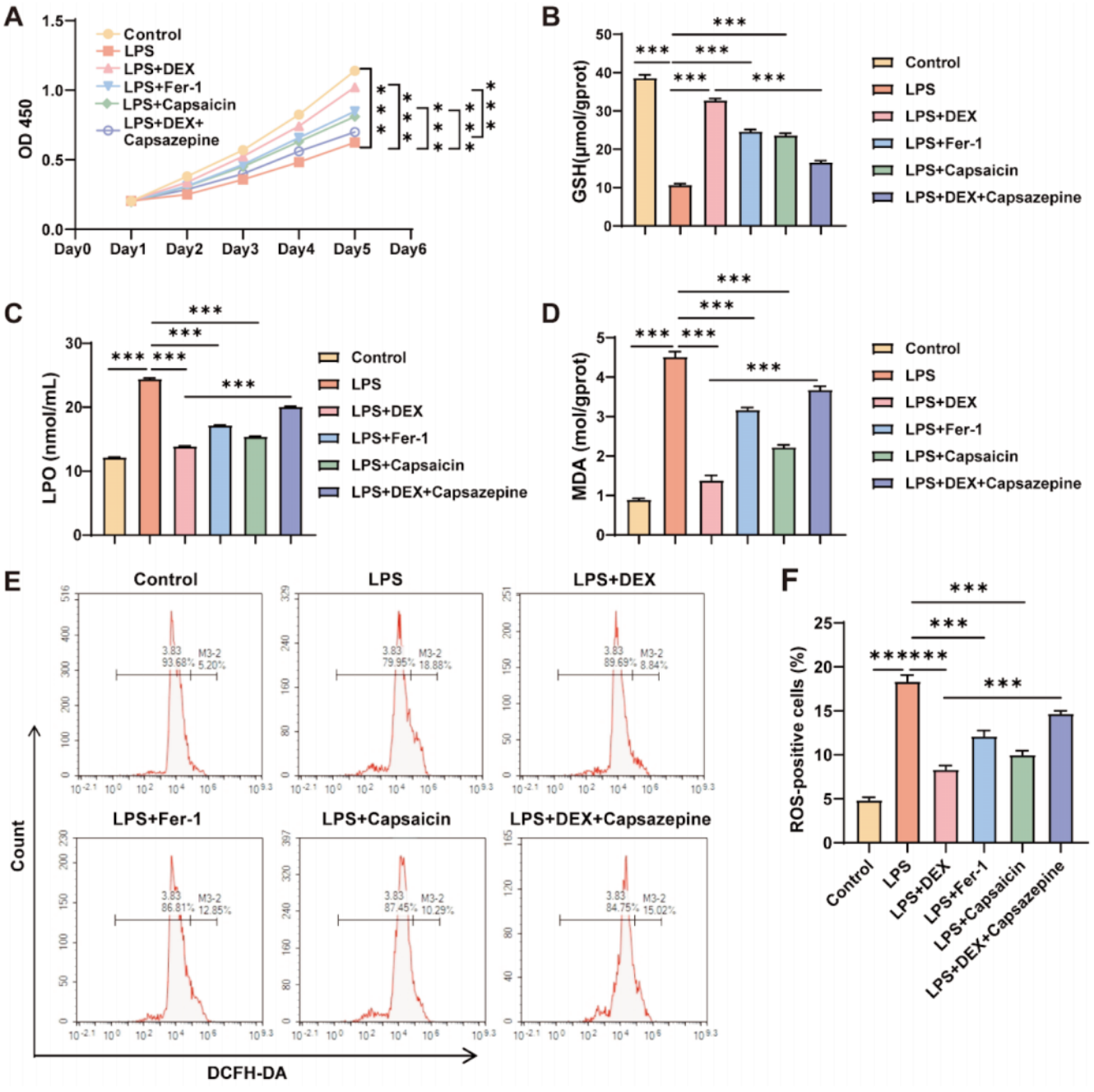

Figure 4. DEX attenuates LPS-induced cell viability loss and oxidative stress, with effects influenced by pharmacological modulation of TRPV1. **A**) Cell viability following treatment with DEX, Fer-1, capsaicin, or DEX plus capsazepine in the presence of LPS. **B**) GSH levels. **C**) LPO levels. **D**) MDA levels. **E**) Representative flow cytometry histograms of DCF fluorescence following DCFH-DA staining. **F**) Quantification of ROS-positive cells (%); Data are presented as mean ±SD (n=3 per group). ***p<0.001.

OPEN ACCESS

component, while the in vivo phenotype may additionally integrate vascular and immune effects.

TRPV1 is a non-selective cation channel expressed in sensory neurons and cardiac tissue, where it can influence calcium handling, oxidative stress, and cardioprotective signaling.[32,33] Capsaicin reproduced several protective effects of DEX, whereas capsazepine partially reduced DEX-associated preservation of cell viability and redox homeostasis. These results support a role for pharmacologically TRPV1-sensitive signaling. The concordant changes in TRPV1 expression, cell viability, and redox measures connect the pharmacological responses to the broader protective phenotype.

Ferroptosis-related injury involves lipid peroxidation, iron accumulation, impaired antioxidant defenses, and mitochondrial alterations.[34-37] DEX reduced LPO, MDA, and Fe^{2+} accumulation, increased GSH levels, preserved mitochondrial morphology,

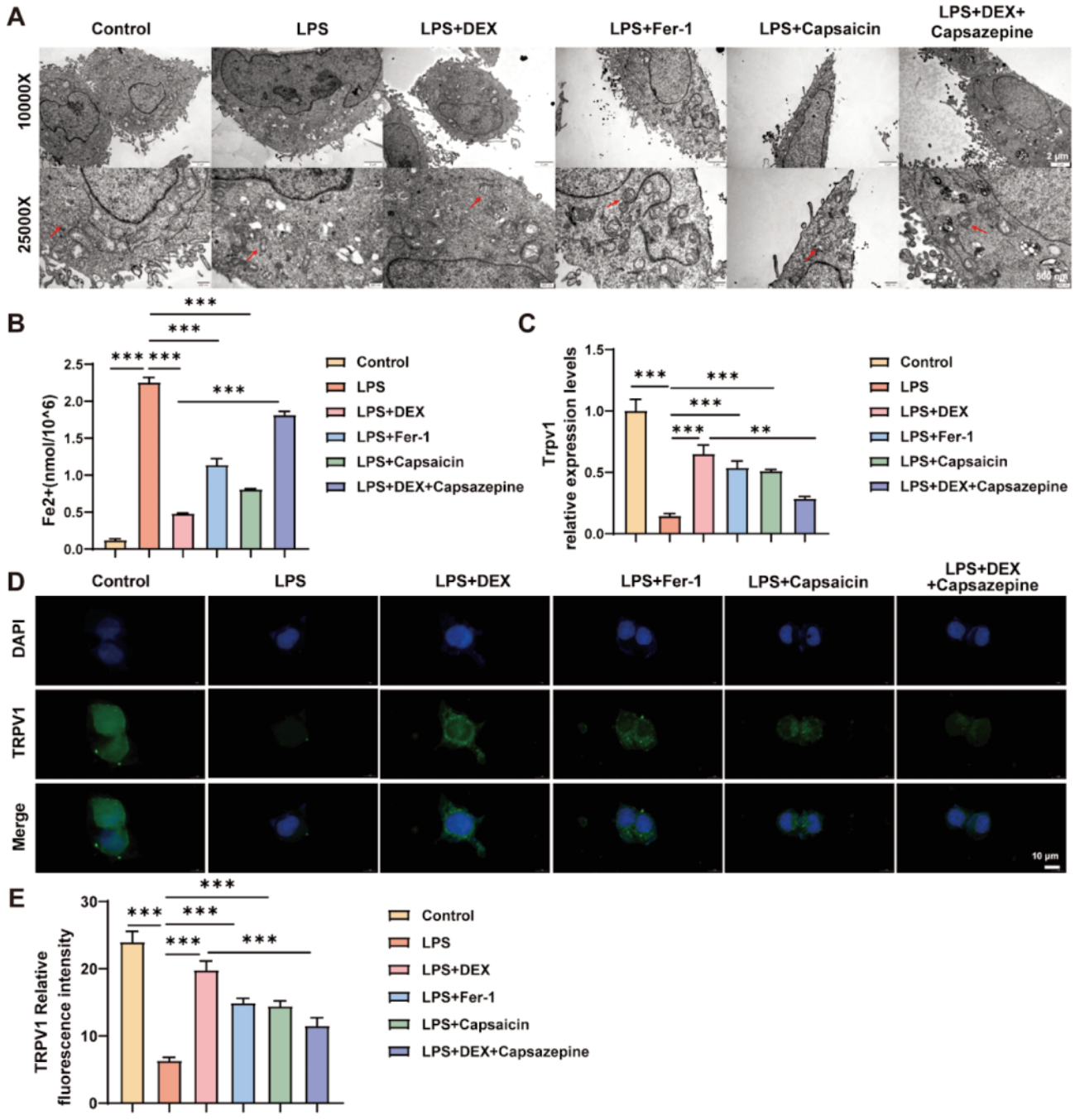

Figure 5. DEX reduces iron accumulation, increases TRPV1 expression, and preserves mitochondrial integrity, with effects influenced by pharmacological modulation of *TRPV1*. **A**) TEM images of mitochondrial structure; at 10,000×, scale bar: 2 μm; at 25,000×, scale bar: 500 nm. **B**) Intracellular Fe^{2+} levels. **C**) TRPV1 mRNA expression. **D**) Representative immunofluorescence images of TRPV1 (green) and nuclei (DAPI, blue); scale bar: 10 μm. **E**) Quantitative analysis of TRPV1 mean fluorescence intensity; Data are presented as mean ±SD (n=3 per group). $^{**}p<0.01$, $^{***}p<0.001$.

increased GPX4 and SLC7A11 expression, and decreased ACSL4 expression. Fer-1 and capsaicin produced overlapping protective effects, whereas capsazepine attenuated several DEX-associated changes. Fer-1 also increased TRPV1 expression, linking TRPV1 regulation to improvements in ferroptosis-related indicators. These coordinated responses support an association between TRPV1 regulation and the protective phenotype, with feedback regulation or a shared upstream response as possible explanations.

Mitochondrial integrity is central to cardiomyocyte homeostasis.[38] Mitochondrial shrinkage, increased membrane density, and loss or reduction of cristae are characteristic ultrastructural features associated with ferroptosis.[10,39] In the present study, DEX, Fer-1, and capsaicin attenuated LPS-associated mitochondrial shrinkage, increased membrane density, and cristae loss, while capsazepine partially reduced the protective phenotype. These ultrastructural findings align with the biochemical and protein evidence of reduced ferroptosis-related changes.

The time-course analysis identified day 2 as the peak injury time point based on the measured cardiac injury and biochemical markers, providing a defined time point for subsequent experiments. DEX was administered before CLP, and the findings therefore characterize its cardioprotective effects in a preconditioning setting. Previous CLP studies have similarly shown that DEX pretreatment attenuates myocardial injury, oxidative stress, iron accumulation, and ferroptosis-related alterations.[14] The present study extends this evidence by integrating cardiac functional and tissue assessments with cellular findings and pharmacological modulation of TRPV1.

The paired animal and cell models provide complementary evidence linking DEX-associated cardioprotection with TRPV1 upregulation and reduced ferroptosis-related injury. The pharmacological findings support TRPV1 involvement, with interpretation informed by the reported TRPV1-independent effects of capsaicin on cardiac ion channels.[40] Genetic manipulation of TRPV1 combined with time-resolved analyses can further define target specificity and regulatory direction. Post-CLP dosing studies can

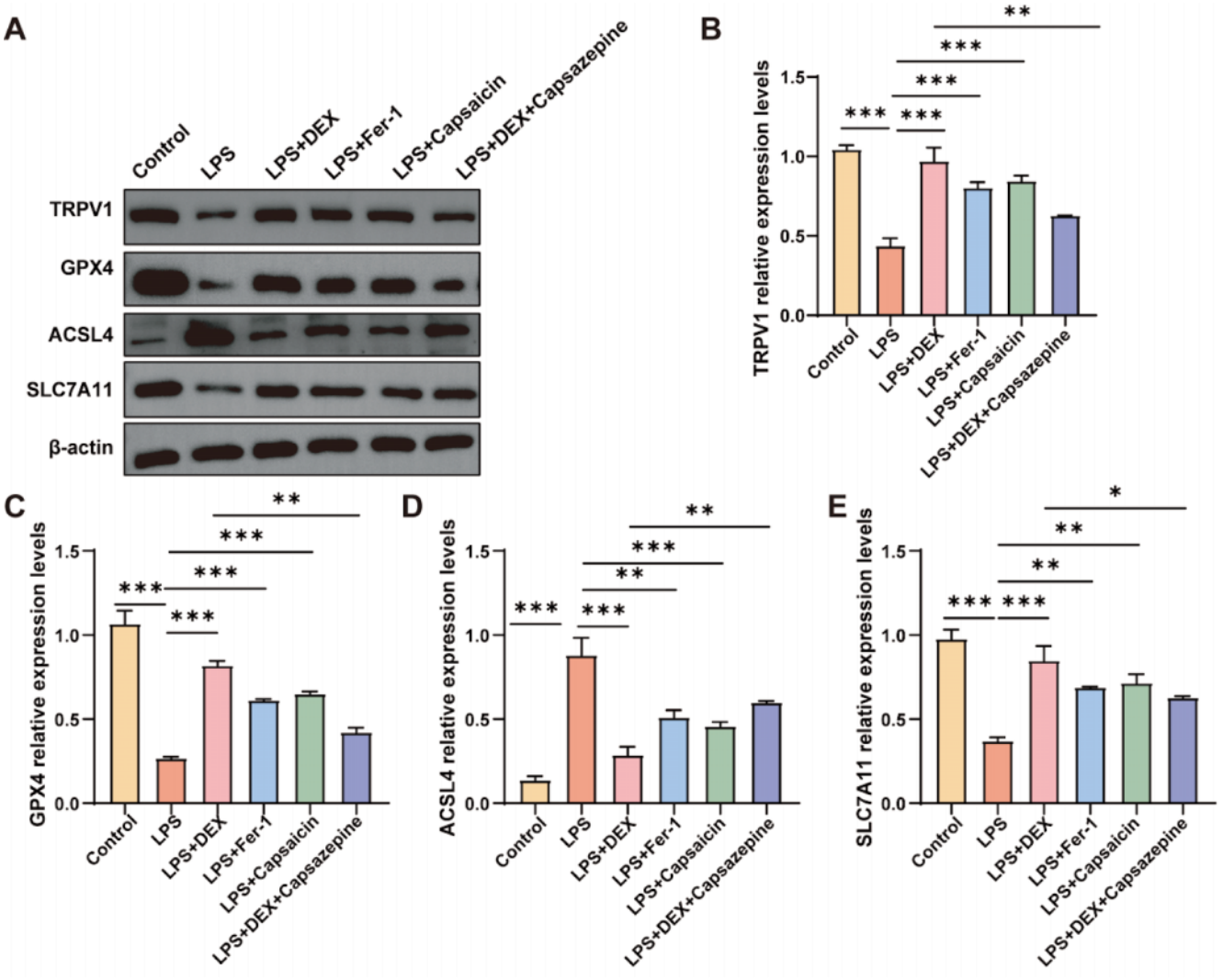

Figure 6. DEX-associated changes in TRPV1 and ferroptosis-related protein expression. Representative Western blots (**A**) and quantitative analyses of TRPV1 (**B**), GPX4 (**C**), ACSL4 (**D**), and SLC7A11 (**E**); Data are presented as mean ±SD (n=3 per group). *p<0.05, **p<0.01, ***p<0.001.

OPEN ACCESS

extend the current preconditioning findings to intervention after sepsis onset.

In summary, DEX pretreatment attenuated CLP-associated myocardial injury and produced concordant protection in LPS-stimulated H9c2 cells. Across both models, the protective phenotype was accompanied by increased TRPV1 expression, improved redox and iron-related measures, and a shift in ferroptosis-related markers. Pharmacological modulation further connects TRPV1-sensitive signaling with this coordinated response.

References

1. Global Burden of Cardiovascular Diseases and Risks 2023 Collaborators. Global, regional, and national burden of cardiovascular diseases and risk factors in 204 countries and territories, 1990-2023. J Am Coll Cardiol 2025;86:2167-43.
2. Beesley SJ, Weber G, Sarge T, Nikravan S, Grissom CK, Lanspa MJ, et al. Septic cardiomyopathy. Crit Care Med 2018;46:625-34.
3. Stanzani G, Duchen MR, Singer M. The role of mitochondria in sepsis-induced cardiomyopathy. Biochim Biophys Acta Mol Basis Dis 2019;1865:759-73.
4. Zhang T, Mei Q, Dai S, Liu Y, Zhu H. Use of dexmedetomidine in patients with sepsis: a systematic review and meta-analysis of randomized-controlled trials. Ann Intensive Care 2022;12:81.
5. Si X, Huang Z, Pan Z. Clinical effects of dexmedetomidine on patients with sepsis and myocardial injury. Medicine 2024;103:e40257.
6. Phan T, Ton H, Hajnalka G, Pórszász R, Tóth A, Russo R, et al. TRPV1 in arteries enables a rapid myogenic tone. J Physiol 2022;600:1651-66.
7. Hurt CM, Lu Y, Stary CM, Piplani H, Small BA, Urban TJ, et al. Transient receptor potential vanilloid 1 regulates mitochondrial membrane potential and myocardial reperfusion injury. J Am Heart Assoc 2016;5:e003774.
8. Randhawa PK, Jaggi AS. TRPV1 channels in cardiovascular system: A double edged sword? Int J Cardiol 2017;228:103-13.
9. Wang L, Wang DH. TRPV1 gene knockout impairs postischemic recovery in isolated perfused heart in mice. Circulation 2005;112:3617-23.
10. Dixon SJ, Lemberg KM, Lamprecht MR, Skouta R, Zaitsev EM, Gleason CE, et al. Ferroptosis: An iron-dependent form of nonapoptotic cell death. Cell 2012;149:1060-72.
11. Yang W, Wang Y, Fu C, Li C, Feng F, Li H, et al. Quantitative visualization of myocardial ischemia-reperfusion-induced cardiac lesions via ferroptosis magnetic particle imaging. Theranostics 2024;14:1081-97.
12. Lu JS, Wang JH, Han K, Li N. Nicorandil regulates ferroptosis and mitigates septic cardiomyopathy via TLR4/SLC7A11 signaling pathway. Inflammation 2024;47:975-88.
13. Liu P, Wang S, Li L, Li R, Fan M, Kong J, et al. TRPV1 inhibits ferroptosis and mitophagy to alleviate heart failure by activating SFXN2. Front Biosci (Landmark Ed) 2025;30:37052.
14. Wang C, Yuan W, Hu A, Li J, Xia Z, Yang CF, et al. Dexmedetomidine alleviated sepsis−induced myocardial ferroptosis and septic heart injury. Mol Med Rep 2020;22:175-84.
15. Xu L, Bao H, Si Y, Wang X. Effects of dexmedetomidine on early and late cytokines during polymicrobial sepsis in mice. Inflamm Res 2013;62:507-14.
16. Zhang P, Peng J, Ren YQ, Zheng H, Yan H. Dexmedetomidine protects against endothelial injury in septic rats induced by cecal ligation and puncture by decreasing angiopoietin 2 and increasing vascular endothelial cadherin levels. Exp Ther Med 2021;21:111.
17. Li J, Xiao F, Lin B, Huang Z, Wu M, Ma H, et al. Ferrostatin-1 improves acute sepsis-induced cardiomyopathy via inhibiting neutrophil infiltration through impaired chemokine axis. Front Cell Dev Biol 2024;12:1510232.
18. Zhang S, Luo N, Wu H, Chen J, Jiang Y, Xiao L, et al. Capsaicin attenuates sepsis−associated encephalopathy by inhibiting neuroinflammation and apoptosis whilst activating mitophagy through the BNIP3/NIX pathway. Mol Med Rep 2025;32:322.
19. Luz-Martínez BA, Viveros-Paredes JM, Rojas-Molina A, Ibarra-Alvarado C. The multitarget antinociceptive compound affinin and its effects on hypothermia, hypolocomotion, and sickness behavior in lipopolysaccharide-treated mice. Molecules 2025;30:2554.
20. Zhuang J, Cheng G, Huang J, Guo H, Lai Y, Wang J, et al. Rosuvastatin exerts cardioprotective effect in lipopolysaccharide-mediated injury of cardiomyocytes in an MG53-dependent manner. BMC Cardiovasc Disord 2022;22:69.
21. Zhu Z, Ling X, Zhou H, Zhang C. Dexmedetomidine at a dose of 1 μM attenuates H9c2 cardiomyocyte injury under 3 h of hypoxia exposure and 3 h of reoxygenation through the inhibition of endoplasmic reticulum stress. Exp Ther Med 2021;21:132.
22. Cai S, Liu Y, Cheng Y, Yuan J, Fang J. Dexmedetomidine protects cardiomyocytes against hypoxia/reoxygenation injury via multiple mechanisms. J Clin Lab Anal 2022;36:e24119.
23. Park T-J, Park JH, Lee GS, Lee J-Y, Shin JH, Kim MW, et al. Quantitative proteomic analyses reveal that GPX4 downregulation during myocardial infarction contributes to ferroptosis in cardiomyocytes. Cell Death Dis 2019;10:835.
24. Hu T, Yu W-P, Wang X-Q, et al. Activation of PPAR-α attenuates myocardial ischemia/reperfusion injury by inhibiting ferroptosis and mitochondrial injury via upregulating 14-3-3η. Sci Rep 2024;14:15246.
25. Sattler K, El-Battrawy I, Cyganek L, Lang S, Lan H, Li X, et al. TRPV1 activation and internalization is part of the LPS-induced inflammation in human iPSC-derived cardiomyocytes. Sci Rep 2021;11:14689.
26. Sun Z, Han J, Zhao W, Zhang Y, Wang S, Ye L, et al. TRPV1 activation exacerbates hypoxia/reoxygenation-induced apoptosis in H9C2 cells via calcium overload and mitochondrial dysfunction. Int J Mol Sci 2014;15:18362-80.
27. Wang Z, Yao M, Jiang L, Wang L, Yang Y, Wang Q, et al. Dexmedetomidine attenuates myocardial ischemia/reperfusion-induced ferroptosis via AMPK/GSK-3β/Nrf2 axis. Biomed Pharmacother 2022;154:113572.
28. He H, Liu P, Li P. Dexmedetomidine ameliorates cardiac ischemia/reperfusion injury by enhancing autophagy through activation of the AMPK/SIRT3 pathway. Drug Des Devel Ther 2023;17:3205-18.
29. Zhao H, Fan M, Zhang J, Gao Y, Chen L, Huang L. Amyloid beta-induced mitochondrial dysfunction and endothelial permeability in cerebral microvascular endothelial cells: The protective role of dexmedetomidine. Brain Res Bull 2025;220:111137.
30. Zhao Q, Yu S, Ling Y, Hao S, Liu J. The protective effects of dexmedetomidine against hypoxia/reoxygenation-induced inflammatory injury and permeability in brain endothelial cells mediated by sigma−1 receptor. ACS Chem Neurosci 2021;12:1940-7.

31. Wang L, Liu J, Wang Z, Qian X, Zhao Y, Wang Q, et al. Dexmedetomidine abates myocardial ischemia reperfusion injury through inhibition of pyroptosis via regulation of miR-665/MEF2D/Nrf2 axis. Biomed Pharmacother 2023;165:115255.
32. Wei J, Lin J, Zhang J, et al. TRPV1 activation mitigates hypoxic injury in mouse cardiomyocytes by inducing autophagy through the AMPK signaling pathway. Am J Physiol Cell Physiol 2020;318:C1018-29.
33. Zhao R, Liu X, Qi Z, Yao X, Tsang S. TRPV1 channels regulate the automaticity of embryonic stem cell−derived cardiomyocytes through stimulating the Na^{+}/Ca^{2+} exchanger current. J Cell Physiol 2021;236:6806-23.
34. Liu D, Cheng X, Wu H, Song H, Bu Y, Wang J, et al. CREG1 attenuates doxorubicin-induced cardiotoxicity by inhibiting the ferroptosis of cardiomyocytes. Redox Biol 2024;75:103293.
35. Zhang W, Lu J, Wang Y, Sun P, Gao T, Xu N, et al. Canagliflozin attenuates lipotoxicity in cardiomyocytes by inhibiting inflammation and ferroptosis through activating AMPK pathway. Int J Mol Sci 2023;24:858.
36. Cai W, Liu L, Shi X, Liu Y, Wang J, Fang X, et al. Alox15/15-HpETE aggravates myocardial ischemia-reperfusion injury by promoting cardiomyocyte ferroptosis. Circulation 2023;147:1444-60.
37. Yuan Y, Mei Z, Qu Z, Li G, Yu S, Liu Y, et al. Exosomes secreted from cardiomyocytes suppress the sensitivity of tumor ferroptosis in ischemic heart failure. Signal Transduct Target Ther 2023;8:121.
38. Murphy E, Ardehali H, Balaban RS, DiLisa F, Dorn GW 2nd, Kitsis RN, et al. Mitochondrial function, biology, and role in disease. Circ Res 2016;118:1960-91.
39. Gao M, Yi J, Zhu J, Minikes AM, Monian P, Thompson CB, Jiang X. Role of mitochondria in ferroptosis. Mol Cell 2019;73:354-363.e3
40. Isaev D, Yang KS, Shabbir W, Howarth FC, Oz M. Capsaicin inhibits multiple voltage-gated ion channels in rabbit ventricular cardiomyocytes in TRPV1-independent manner. Pharmaceuticals (Basel) 2022;15:1187.

Received: 6 July 2026. Accepted: 12 October 2026.

This work is licensed under a Creative Commons Attribution-NonCommercial 4.0 International License (CC BY-NC 4.0).
©Copyright: the Author(s), 2026
Licensee PAGEPress, Italy
European Journal of Histochemistry 2026; 70:4732
doi:10.4081/ejh.2026.4732

Publisher's note: all claims expressed in this article are solely those of the authors and do not necessarily represent those of their affiliated organizations, or those of the publisher, the editors and the reviewers. Any product that may be evaluated in this article or claim that may be made by its manufacturer is not guaranteed or endorsed by the publisher.

OPEN ACCESS